Residue Ionization and Ion Transport through OmpF Channels

Ekaterina M. Nestorovich, Tatiana K. Rostovtseva, and Sergey M. Bezrukov
Laboratory of Physical and Structural Biology, National Institute of Child Health and Human Development, National Institutes of Health, Bethesda, Maryland

ABSTRACT   Single trimeric channels of the general bacterial porin, OmpF, were reconstituted into planar lipid membranes and their conductance, selectivity, and open-channel noise were studied over a wide range of proton concentrations. From pH 1 to pH 12, channel transport properties displayed three characteristic regimes. First, in acidic solutions, channel conductance is a strong function of pH; it increases by approximately threefold as the proton concentration decreases from pH 1 to pH 5. This rise in conductance is accompanied by a sharp increase in cation transport number and by pronounced open-channel low-frequency current noise with a peak at ~pH 2.5. Random stepwise transients with amplitudes at ~1/5 of the monomer conductance are major contributors to this noise. Second, over the middle range (pH 5 ÷ pH 9), channel conductance and selectivity stay virtually constant; open channel noise is at its minimum. Third, over the basic range (pH 9 ÷ pH 12), channel conductance and cation selectivity start to grow again with an onset of a higher frequency open-channel noise. We attribute these effects to the reversible protonation of channel residues whose pH-dependent charge influences transport by direct interactions with ions passing through the channel.

INTRODUCTION

Despite approximately 25 years of extensive studies, bacterial porins are still at the center of researchers' attention (e.g., Delcour, 2003, 2002; Bredin et al., 2002; Robertson and Tieleman, 2002a,b; Im and Roux, 2002; Philippsen et al., 2002; Rostovtseva et al., 2002; Phale et al., 2001; Koebnik et al., 2000; Van Gelder et al., 2000; Chevalier et al., 2000; Simonet et al., 2000). Physical mechanisms underlying important properties of these channels, such as ion and neutral solute selectivity (Klebba and Newton, 1998) and the voltage- and pH-induced "gating" of major proteins from the outer membrane of *Escherichia coli* OmpF, OmpC, and PhoE (Van Gelder et al., 1997; Phale et al., 1997; Bainbridge et al., 1998a,b; Müller and Engel, 1999) are poorly understood. Since bacteria survival requires a continuous exchange of solutes across the cell wall, insights into the transport properties of porins are crucial for the successful manipulation of bacterial activity (Chevalier et al., 2000; Simonet et al., 2000). The latest single-molecule studies with porins reconstituted into planar lipid membranes (Bezrukov et al., 2000; Kullman et al., 2002; Nestorovich et al., 2002) demonstrated the principal possibility to study a number of transport processes involved in the basic cellular mechanisms with unprecedented molecular details. Combined with the availability of high-resolution three-dimensional porin structures (Weiss et al., 1990; Cowan et al., 1992; Kreusch and Schultz, 1994) and recent progress in Brownian dynamics simulations (Robertson and Tieleman, 2002b; Im and Roux, 2002; Phale et al., 2001, 1998; Im et al., 2000; Schirmer and Phale, 1999; Suenaga et al., 1998; Tieleman and Berendsen, 1998; Watanabe et al., 1997), these studies advance our understanding of physical principles involved in the channel-facilitated solute transport.

OmpF is one of the major general diffusion porins from the outer membrane of *E. coli* (Nikaido and Vaara, 1985). Reconstituted into planar lipid bilayers, OmpF forms large homotrimeric channels (Benz et al., 1978; Schindler and Rosenbusch, 1978), which correspond to natural OmpF organization. The relative nonspecific molecular sieve properties (for review see Nikaido, 1992), the slight cationic selectivity (Benz et al., 1979; Kobayashi and Nakae, 1985), voltage- (Schindler and Rosenbusch, 1978, 1981), and pH-induced (Todt et al., 1992) "gating" of OmpF have been studied extensively. Understanding porin permeability for nutrients (Benz and Bauer, 1988) and antibiotics (Yoshimura and Nikaido, 1985) is crucially important for biotechnological and medical applications. However, even with the three-dimensional structure of OmpF known for more than 10 years (Cowan, et al., 1992), the molecular mechanisms of this porin functioning have yet to be revealed.

New methods developed for investigations of metabolite and other large-molecule transport at the single-channel level (Bezrukov et al., 1994; Kasianowicz et al., 1996; Rostovtseva and Bezrukov, 1998; Bezrukov, 2000; Nestorovich et al., 2002; Meller and Branton, 2002; Meller, 2003) require the detailed knowledge of noise characteristics of the open single channels. Appreciation of noise generation mechanisms in nanoscale objects is also important for the successful development of single-molecular sensors based on natural ion channels (Bayley and Cremer, 2001) and solid-state micro- and nanostructures (Li, et al., 2001; Saleh and Sohn, 2003).

The water-filled pore of each monomer in the OmpF trimer has an asymmetrical shape with a narrow (~7 Å × 11 Å) constriction zone at approximately one-half the height of the channel (Cowan, et al., 1992). Negatively and positively

charged residues in the constriction zone create a strong transverse electrostatic field inside the channel. Because the charge state of the residues changes with solution acidity, the strength of this field is pH-dependent. The changing field can change channel conductance by direct interactions with permeant ions or by changing the channel geometry due to the shift of the internal loop at the constriction zone. Channel residue protonation is a reversible dynamic process with a characteristic time spanning the range of micro- and milliseconds that is attainable in single-channel experiments (Prod'hom et al., 1987; Hess et al., 1989; Bezrukov and Kasianowicz, 1993; Kasianowicz and Bezrukov, 1995; Rostovtseva et al., 2000). Therefore, both the direct interactions of fluctuating residue charges with penetrating ions and the possible loop displacement can result in measurable conductance fluctuations.

The effect of pH on porin voltage gating (Xu et al., 1986; Todt et al., 1992; Saint et al., 1996; Liu and Delcour, 1998) and conductance (Benz et al., 1979; Xu et al., 1986; Todt and McGroarty, 1992; Todt et al., 1992) has been addressed repeatedly. It is well established that acidic pH makes porins more easily gated by applied voltage (for a recent discussion see Delcour, 2003). Interestingly, reconstitution experiments (Benz et al., 1979; Xu et al. 1986) but not patch clamp data (Liu and Delcour, 1998) showed a decrease in channel conductance at increasing solution acidity.

In the present study we analyze several OmpF channel characteristics over a wide range of solution acidities in its fully open, "nongated" state. Varying solution pH from pH 1 to pH 12, we characterize the following channel properties: 1), average conductance; 2), ion selectivity; 3), time-resolved discrete conductance fluctuations; and 4), open channel noise. We find that channel conductance, noise, and ion selectivity display three characteristic regimes. At neutral pH, conductance and selectivity are only weakly dependent on solution acidity and open channel noise is at its minimum (though exceeding thermal and shot-noise power spectral density at low frequencies by ~30 or more times at 100 mV). In acidic solutions channel conductance and cation selectivity decrease sharply; at pH 1 conductance falls to approximately one-third of its value at neutral pH and at pH 3.5 it goes through a well-defined peak at ~pH 2.5. In basic solutions, at pH values exceeding pH 9, the channel conductance increases with respect to its value at neutral pH. Cationic selectivity and noise increase too.

We find that multiple ionization processes with different relaxation times are responsible for the observed changes in channel ion conductance and selectivity. Some of them can be resolved as stepwise conductance changes; the others are too fast and can only be seen as high-frequency components in the power spectra of the open channel noise. Polymer partitioning experiments are in favor of direct interactions between the pH-dependent charge of ionizable residues and the permeant ions as the main cause of these effects.

MATERIAL AND METHODS

Wild-type OmpF was a generous gift of Dr. Mathias Winterhalter. The following chemical reagents were used in this study: KCl, KOH, and HCl (Mallinckrodt, St. Louis, MO); 2M CaCl$_2$ (Quality Biological, Gaithersburg, MD); ultrol grade MES or HEPES (Calbiochem, San Diego, CA); "purum" hexadecane (Fluka, Buchs, Switzerland); 1,2-diphytanoyl-sn-glycero-3-phosphatidylcholine (Avanti Polar Lipids, Alabaster, AL); pentane (Burdick and Jackson, Muskegon, MI); agarose (Bethesda Research Laboratory, Gaithersburg, MD). Doubly distilled and deionized water was used to prepare solutions. All solutions after preparation were purified by filtration through a 0.45-μm filter.

"Solvent-free" planar lipid bilayers were formed from the monolayers made from 5 mg/ml solution of DPhPC in pentane on a 60-μm-diameter aperture in the 15-μm-thick Teflon film that separated two (cis and trans) compartments of the Teflon chamber (Bezrukov and Vodyanoy, 1993; after Montal and Mueller, 1972). The aperture was pretreated with 1% solution of hexadecane in n-pentane and dried during 15 min before membrane formation. The film and the total capacitances were close to 25 and 50 pF, respectively.

The electrical potential difference across the bilayer was applied with a pair of Ag-AgCl electrodes in 3 M KCl, 15% agarose bridges. Potential was determined as positive when it was greater at the side of OmpF addition (cis-side). The signal amplification, filtration, and analysis techniques were previously described elsewhere (Rostovtseva et al., 2002). Solution conductivities were measured using a CDM 83 conductivity meter (Radiometer, Copenhagen, Denmark) at 23.0°C. All experiments were carried out at room temperature of 23 ± 2°C.

Single channels were formed by adding (0.1 ÷ 0.3) μl of 1 μg/ml stock solution of OmpF to 1.5 ml aqueous phase in the cis half of the chamber while stirring at –(180 ÷ 200) mV of applied voltage for ~5 min. Measurements were carried out in solutions containing 1 mM CaCl$_2$ with KCl concentration equal to 0.1 or 1 M at pH 1 ÷ pH 12. Solutions were buffered by MES or HEPES with a final concentration of 5 mM. Stock solution pH was adjusted by adding KOH or HCl. Control experiments at pH 5 ÷ pH 6 in the absence of any buffers showed no dependence of the OmpF properties (conductance and open channel noise) on the buffer nature.

In most of the experiments, the acidity of membrane-bathing solutions was being changed while recording ion current from the same single channel. To attain different pH, proper amounts of similar solutions with lower or higher pH values were admixed to the bathing aqueous phases. The pH was monitored during the experiment after each single admixing by taking 0.4 ml samples from both compartments of the chamber (pH/Ion Meter 450, Corning, Corning, NY). This way we were able to analyze characteristics of an individual channel at different experimental conditions, thus minimizing errors from a slight natural spread in the properties from channel to channel.

The cation-anion selectivity was analyzed by measuring zero current potential, E_{rev}, under conditions of a 10-fold gradient of KCl concentration across the bilayer. The cationic transport number (t_K^+), related to the anionic transport number (t_{Cl}^-) by $t_K^+ + t_{Cl}^- = 1$, was calculated using (e.g., see Urban et al., 1980),

$$E_{rev} = \left(1 - 2t^+\right)\frac{kT}{e}\ln\frac{a_{1M}}{a_{0.1M}},$$

where a_{1M} and $a_{0.1M}$ are KCl activities respectively in 1 M (cis side) and 0.1 M (trans side) solutions and k, T, and e have their usual meaning of the Boltzmann constant, the absolute temperature, and the electron charge.

RESULTS AND DISCUSSION

Because the nature of things is sometimes better revealed by the examination of extreme cases, we have analyzed the

properties of the single OmpF channel over a wide, "non-physiological" pH range.

Fig. 1 shows single OmpF channel recordings at pH 3.9 (*A*), pH 5.5 (*B*), and pH 8.0 (*C*). These recordings illustrate a well-known correlation between voltage and pH-induced channel closure (Schindler and Rosenbusch, 1981; Todt et al., 1992; Xu et al., 1986; Saint et al., 1996). Being rather stable at ±100 mV of applied voltage at pH 8.0 (note only a few transients from the fully open channel to two-thirds of the total conductance in Fig. 1 *C*), the channel is easily closed by this voltage when solution pH is shifted to subacid values (Fig. 1 *A*). Despite the relative stability of OmpF at pH values close to neutral, an increase of applied voltage leads to a similar voltage-induced closure (e.g., see Fig. 1 in Rostovtseva et al., 2002). We used this characteristic three-step closure as a test for the channel trimeric organization, especially under extreme pH conditions. In the present article we address the transport properties of the OmpF channel in its fully open, "nongated" conformation.
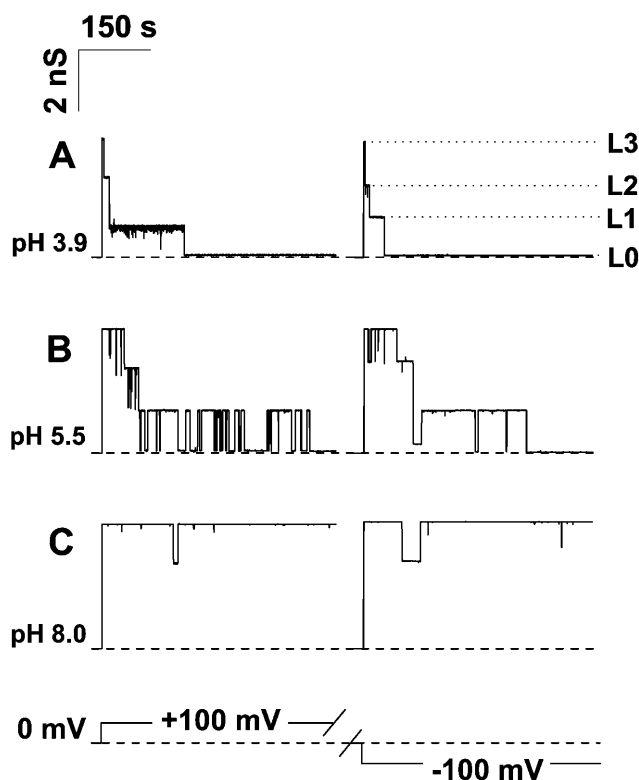

FIGURE 1 Typical tracks of ion conductance for single trimeric OmpF channels reconstituted into planar lipid membranes at pH 3.9 (*A*), pH 5.5 (*B*), and pH 8.0 (*C*) demonstrate that voltage-induced channel closure is facilitated by low pH. The membrane was formed from DPhPC, the membrane bathing solutions contained 1 M KCl and 5 mM HEPES or MES. Time averaging was 100 ms. The dashed lines show zero current levels, the dotted lines in *A* designate a fully open state (*L3*, all thee monomers open), and two partially closed states (*L2*, two monomers open; *L1*, one monomer open). Note the presence of residual conductance (*L0*) after the total three-step closure (*A*, *B*).

Ion conductance and ion selectivity

Asymmetry in the OmpF structure and in the positions of charges inside the channel lumen leads to asymmetry in channel current-voltage characteristics. Fig. 2 illustrates voltage dependence of the average conductance in 1 M and 0.1 M KCl at pH 8.0 and pH 3.9. Because the channel conductance fluctuates in a pH-dependent manner (see below), the experimental points represent averages over time intervals of 1–3 s. Interestingly, the conductance-voltage curves have differing asymmetry depending on solution pH. At pH 8.0 the channel conductance is higher at −200 mV than at +200 mV, whereas at pH 3.9 the opposite is true. The difference is much more pronounced at the smaller salt concentration. While in 1 M KCl this difference is ∼5% (pH 8) and 8% (pH 3.9) only, in 0.1 M KCl it reaches 40% (pH 8) and 12% (pH 3.9). This asymmetry was used as a control of the insertion direction. The infrequent cases (∼3%) of "wrongly" oriented insertions were excluded from our analysis. Which particular orientation is favored by our reconstitution procedure, the one where the extracellular loops of the channel face the *trans*-side of the membrane or the opposite one, is not clear. At the moment, our only conclusion is that one of these orientations predominates.

The channel average conductance as a function of pH is shown in Fig. 3 *A* for −100 mV (*unfilled circles*) and 100 mV (*solid circles*). It summarizes data obtained from four independent single-channel experiments where solution
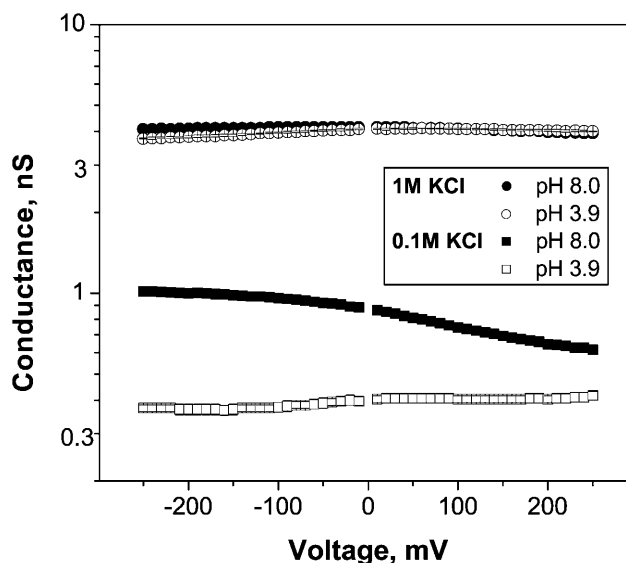

FIGURE 2 Average conductance of a fully open channel as a function of applied voltage for different bathing solution concentrations: 1 M KCl (*circles*) and 0.1 M KCl (*squares*) at pH 8 (*solid symbols*) and pH 3.9 (*unfilled symbols*). Note that the curves have different asymmetry depending on the solution pH. When the voltage changes from −200 mV to 200 mV, the channel conductance grows at pH 3.9 and decreases at pH 8 for both KCl concentrations. Each curve was obtained as a result of averaging of conductance-voltage characteristics for 3–4 independent experiments with different channels.
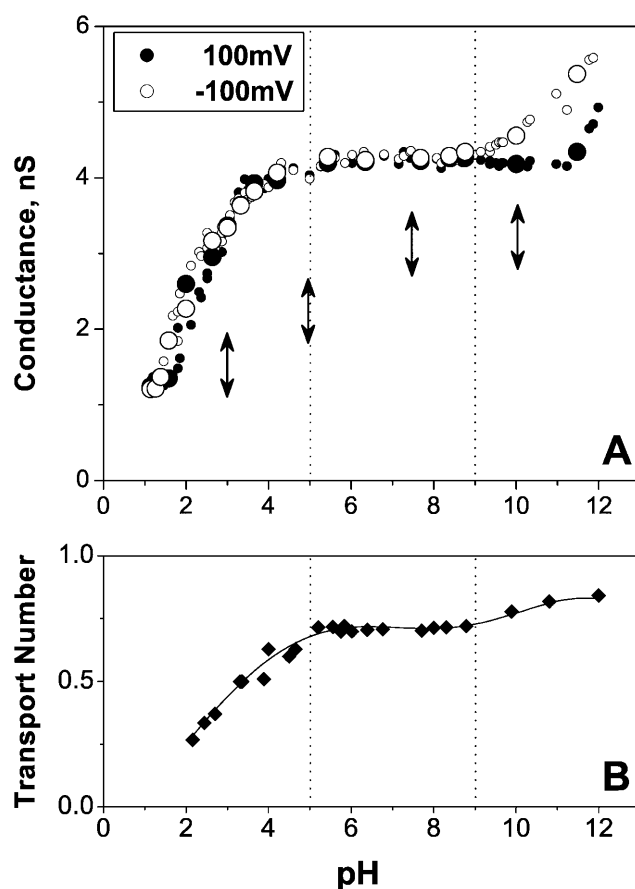
FIGURE 3 (*A*) Average conductance of a fully open channel drops by a factor of 4 when bathing solution pH is shifted from pH 12 to pH 1. This is true for both positive (*solid circles*, 100 mV) and negative (*unfilled circles*, –100 mV) voltages. The data were obtained in four independent experiments with four different single channels. Only one channel was reconstituted in each case. Vertical arrows show initial pH values used for insertions. For example, enlarged circles show the data for the channel inserted at pH 10. Bathing solutions concentration was 1 M KCl. Dashed lines separate three regions of conductance behavior. (*B*) Ion selectivity of a fully open single channel, given as potassium transport number, t^+, depends on solution pH. Three regions can be distinguished in the potassium transport number versus pH curve. The middle region (pH 5–pH 9) shows a constant, slightly cationic selectivity of OmpF; the "acidic" region demonstrates a gradual decrease of cationic selectivity and its inversion to anionic one. The "basic" region displays some growth in cationic selectivity.

acidity was being changed while monitoring the conductance of the same single channel. To examine possible memory effects of the insertion pH, we reconstituted these four channels at four different pH values marked with vertical arrows. For example, the enlarged circles present data obtained from the experiment where the channel was initially inserted at pH 10 marked by the rightmost arrow. No significant difference in the dependence of conductance on solution acidity could be detected for channels inserted at pH 3.0, pH 5.0, pH 7.5, and pH 10.

Channel conductance is an increasing function of pH with the total conductance change of approximately fourfold over

the pH range from 1 to 12. Three different regions of the dependence are clearly seen. The most extended one corresponds to the dependence plateau, which spans over four orders of proton concentration from pH 5 to pH 9. Here the OmpF conductance increase does not exceed 10%.

The second region belongs to low pH (pH 1 ÷ pH 5) and corresponds to the most dramatic conductance change from ~1.3 nS to ~4.1 nS. Importantly, this pH-induced conductance change was found to be fully reversible. To check against the possibility of irreversible denaturation of OmpF by acidic environment, we carried out a specially designed experiment where solution pH had been shifted from pH ~ 4.6 to pH ~ 1.0 and back several times. Complete reproducibility of the conductance readings was observed.

The third region belongs to basic solutions (pH > 9) and shows 15–30% conductance increase depending on the applied voltage. The effect of pH on channel conductance is especially voltage-dependent over this region. At negative voltages the increase starts at lower pH values and is more pronounced.

If the changes in the average conductance are caused by direct interaction of the permeating ions with the pH-dependent charge of the channel residues, one should expect pronounced changes in channel ionic selectivity. This is exactly what we observe. Fig. 3 *B* shows that potassium transport number, t_K^+, measured for the 10-fold salt gradient as described in Material and Methods, is indeed modified by solution pH. Here again one can see three well-defined regions at approximately same pH intervals as before. Over the pH range from 5 to 9, where OmpF conductance is practically constant, OmpF shows pH-independent cation selectivity with $t_K^+ \approx 3t_{Cl}^-$. The sharp decrease in OmpF conductance in acidic solutions is accompanied by a significant drop in t_K^+. At pH 3.5 OmpF shows equal selectivity to cations and anions and at lower pH channel even reverses its selectivity to the anionic one. Finally, the increase of channel conductance at basic pH is accompanied by an increase in cationic selectivity.

Fluctuations and noise in the open state

Residue protonation kinetics are sometimes slow enough to be either resolved as current steps in single-channel experiments (Prod'hom et al., 1987) or measured by noise analysis (Bezrukov and Kasianowicz, 1993; Kasianowicz and Bezrukov, 1995; Rostovtseva et al., 2000). Fig. 4 shows high-resolution (0.1 ms) single open channel recordings for six different pH values from pH 11.8 to pH 2.6. The current through OmpF changes with pH in two different ways. First, both its average and maximal values decrease when solution acidity is increased. Second, we observe pH-dependent fluctuations in the current. At pH values close to neutral (Fig. 4, *B* and *C*) these fluctuations are at their minimum. In basic solutions (Fig. 4 *A*) fast current fluctuations are present but the characteristic time of these fluctuations is too small for
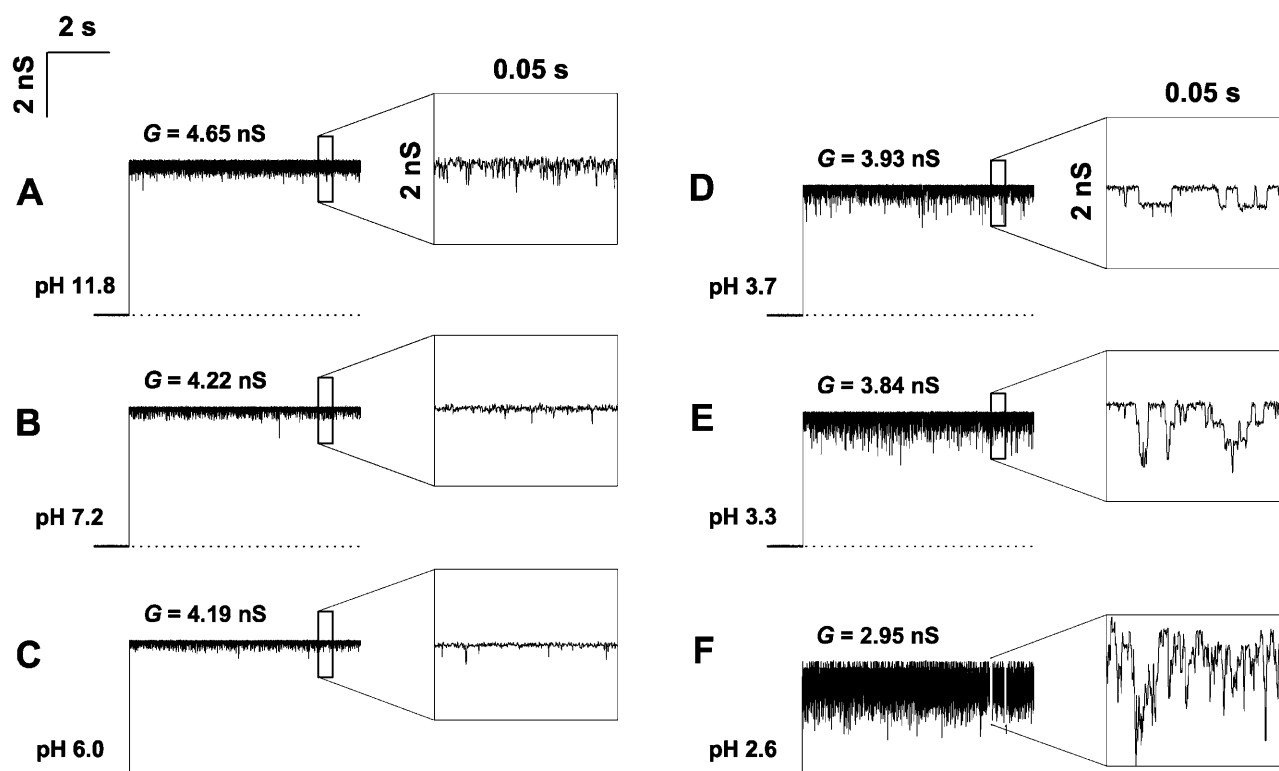
FIGURE 4 Changing pH changes ion current through a fully open channel in at least two ways. First, the increase in proton concentration decreases both the average current and the maximum current, measured using 0.1-ms averaging. Second, it changes the character of current fluctuations. At pH values close to neutral, (*B* and *C*) ion current is most stable and only rare fast downward transients are seen at a finer timescale of the insets on the right. Low pH (*D*) considerably increases intensity of the open channel noise; stepwise current transients with the amplitude corresponding to ~1/5 of one monomer conductance are easily resolved (*inset*). Further solution acidification increases the frequency of these transients (*E* and *F*) decreasing the average conductance of the fully open channel. At pH 2.6, the maximum conductance is also decreased by ~20% in comparison with neutral pH (data in *F* versus data in *B*). In basic solutions (*A*) channel conductance is higher than at neutral pH. Current noise increases at high pH, but the time-resolved stepwise current transients are not observed (*inset*). Recordings were obtained in 1 M KCl bathing solution under 100 mV of applied voltage. Time resolution for all graphs was 0.1 ms.

the elementary events to be resolved. In acidic solutions (Fig. 4, *D* and *E*) the transient lower conductance substates of $0.5 \div 4$ ms average duration can be easily resolved. The frequency of these stepwise transients increases with the increase in solution acidity. At pH values <3.0 there are too many of them to be clearly resolved (Fig. 4 *F*).

Conductance histograms of the transient ''flickering'' to the lower conductance substates for three different solution acidities, pH 4.6, pH 3.7, and pH 3.3, are shown in Fig. 5. The histograms were calculated from the difference between the current of the fully open channel and the current of the lower conductance substates. First, a visual examination of the records was used to find the stepwise changes, and then the current within the substate was averaged over a 1-ms time interval. We have found that at moderate acidities, where the single stepwise changes in conductance are clearly resolvable (Fig. 4, *D* and *E*), there are two characteristic substates. At pH 4.6 they correspond to conductances that are smaller than conductance of the fully open channel by 0.26 nS and 0.30 nS (Fig. 5 *A*). Taking into account conductance of the fully open channel at this pH , this corresponds to 19% and 21% decrease in the current through a channel *monomer*. We attribute the

appearance of these conductance substates to the reversible protonation of two (or more) different residues in the channel constriction zone.

In more acidic solutions the amplitudes of the steps are decreased. At pH 3.7 (Fig. 5 *B*) they are 0.23 nS and 0.26 nS; at pH 3.3 they go down to 0.21 nS and 0.24 nS (Fig. 5 *C*). This decrease is accompanied by the decrease in the maximal conductance of the fully open channel so that the relative conductance decrease per single protonation per monomer are approximately conserved.

Within the accuracy of our experiments the relative areas under the two peaks seem to be pH-independent. The absolute number of the transients per second rapidly increases with the solution acidity (see below); however, over the pH range of 4.6–3.3 where the transients are resolvable, the ratio of their frequencies stays close to 3 in favor of the larger conductance step. In particular, for pH 4.6 this ratio is 2.9 ± 0.5, for pH 3.7 it is 3.2 ± 0.3, and for pH 3.3 it is 3.5 ± 1.4.

Fig. 6 shows power spectral densities of current fluctuations for a single open OmpF channel at different pH values for $+100$ mV of applied voltage in comparison to the spectrum of the background noise. The background noise
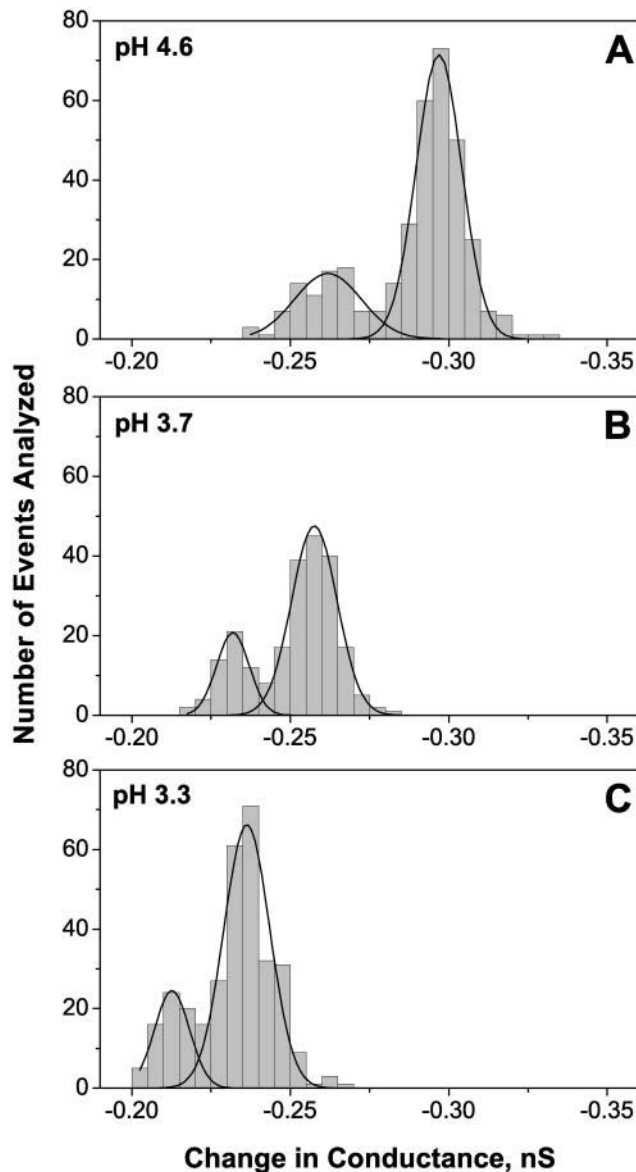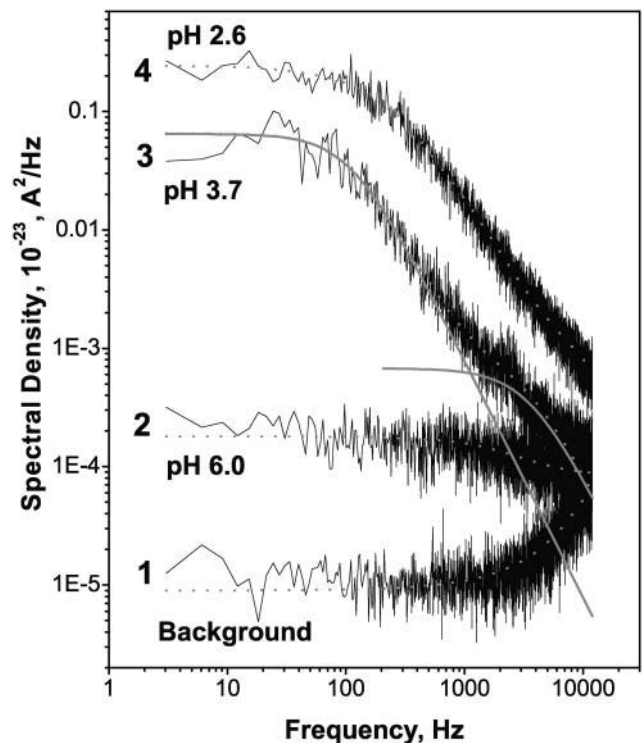
FIGURE 6 Power spectral density of noise in the current through a single fully open channel increases as pH of 1 M KCl solution is shifted to lower values. Background spectrum (*curve 1*) was measured for the membrane with a single OmpF channel at 0 mV. The low-frequency noise of the channel at pH 6.0 (*curve 2*) is orders-of-magnitude smaller than the noise of the same channel at pH 3.7 (*curve 3*). At $f < 500$ Hz the spectra of low-pH fluctuations can be approximated by single Lorentzians (shown for *curve 3*). Except for the background spectrum, the applied voltage was 100 mV.

FIGURE 5 Conductance histograms of the time-resolved stepwise transients induced by low pH (Fig. 4) at pH 4.6 (*A*), pH 3.7 (*B*), and pH 3.3 (*C*). Two peaks on each curve correspond to two clearly defined smaller conductance substates. The amplitudes of these peaks are equal to (0.26 ± 0.02) nS and (0.30 ± 0.01) nS for pH 4.6, (0.23 ± 0.01) nS and (0.26 ± 0.01) nS for pH 3.7, and (0.21 ± 0.01) nS and (0.24 ± 0.01) nS for pH 3.3. Within the statistical error, the ratio of areas under the peaks is independent of solution pH.

was measured at zero transmembrane voltage. It is seen that the spectral characteristics of open channel current fluctuations strongly depend on solution acidity. At low pH values (pH 3.7 and pH 2.6) the channel stepwise flickering to smaller conductance substates dominates the spectra. The characteristic relaxation time of this flickering is ~0.5 ÷ 4 ms depending on the applied voltage and solution pH. In neutral solutions (pH 6.0) the dominant component corresponds to a faster process with the characteristic time

of ~50 μs. Decreasing solution pH sharply increases the spectral density of current noise due to onset of the stepwise flickering, but the contribution from the faster process also grows. Indeed, decomposition of the spectrum obtained at pH 3.7 (*curve 3*) into two Lorentzians (*solid smooth lines*) shows an increase in the amplitude of the faster process.

It is seen that power spectra of the slow stepwise flickering can be satisfactorily approximated by single Lorentzians and, therefore, it is reasonable to model the dynamics of the smaller conductance substates (Fig. 4, *D* and *E*) by two-state Markov processes. This also means that the two substates (Fig. 5) have close relaxation times. The spectrum for each process can be written as

$$S(f) = \frac{4(\Delta i)^2 \tau^2}{\tau_1 + \tau_2} \frac{1}{1 + (2\pi f \tau)^2}, \qquad (1)$$

where f is the frequency, and Δi is the change in the current between the state of maximum conductance of the fully open channel and a substate corresponding to a residue being protonated. The characteristic relaxation time (or correlation time) of the process is defined by

$$\tau = \frac{\tau_1 \tau_2}{\tau_1 + \tau_2}, \tag{2}$$

where τ_1 and τ_2 are the mean lifetimes in protonated and deprotonated states, respectively. These times can be expressed in terms of rate constants k_{on} and k_{off} as

$$\tau_1 = 1/k_{off} \quad \text{and} \quad \tau_2 = (k_{on}[H^+])^{-1} = 10^{pH}/k_{on}, \tag{3}$$

so that, in principle, this kind of analysis is able to provide all the kinetic constants plus the number of independent residues participating in the process (Bezrukov and Kasianowicz, 1993; Kasianowicz and Bezrukov, 1995). However, in the present case this analysis is seriously complicated by the pH dependence of the current change itself: $\Delta i \equiv \Delta i$ (pH). This dependence can be recovered only for the small rate of flickering events in the beginning of the pH-induced decrease in conductance (compare Fig. 3 A and Fig. 4, D–F).

The noise intensity at low frequencies, or "zero-frequency spectral density," $S(0)$, is shown in Fig. 7. It was obtained from the single-Lorentzian analysis, examples of which are given in Fig. 6. The background measured at 0 mV applied voltage was subtracted. The inset in Fig. 7 shows the spectral density at neutral and basic pH at a finer scale. The channel flickering to substates dominates noise spectra in acidic solutions. In 1 M KCl, there is a pronounced and clearly defined peak at ~pH 2.5. Interestingly, lowering bathing solution concentration from 1 M to 0.1 M KCl results in
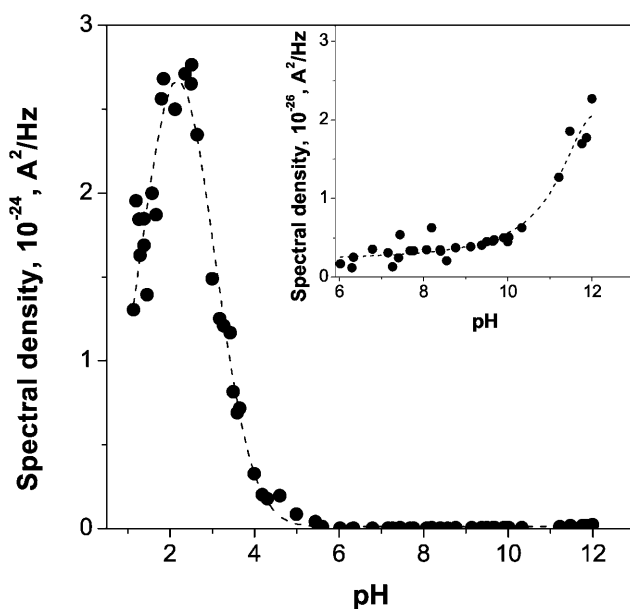

FIGURE 7 The low-frequency spectral density of current noise versus pH dependence has a pronounced peak at ~pH 2.5. Noise at the maximum exceeds noise at neutral pH by approximately three orders of magnitude. As pH is shifted from 6 to 9 (*inset*), the noise stays at its lowest; however, subsequent pH increase leads to the increase in noise spectral density. The spectral density of the background (*curve 1* in Fig. 6) was subtracted. Applied voltage was 100 mV. 1 M KCl was used as a bathing solution.

a significant shift of this peak: it has a maximum at pH close to 4 (data are not shown).

The most considerable increase of the noise (interval from pH 5 to pH 2.5) coincides with the most dramatic pH-dependent change in the average channel conductance (Fig. 3 A). This kind of empirical behavior has been reported and analyzed quantitatively, using simple Markov models, for the α-hemolysin channel (Bezrukov and Kasianowicz, 1993; Kasianowicz and Bezrukov, 1995) and VDAC (Rostovtseva et al., 2000).

The co-existence of at least two distinctly different protonation processes with slow kinetics and an additional faster protonation process, seen as a wide-band noise component, introduces further complications. For this reason we restrict our quantitative analysis only to the pH range from pH 2.5 to pH 5.3.

Fig. 8 A shows the characteristic relaxation time τ for the low-pH stepwise flickering as a function of solution pH. Note a decrease of the characteristic time when pH is shifted from 5.3 to 3 and its saturation at lower pH. This behavior is rather peculiar in comparison with the simple protonation reactions that were found for α-hemolysin channel (Kasianowicz and Bezrukov, 1995). It can be tentatively explained by pronounced interactions between different residues whose charge is pH-dependent. An alternative explanation would be that the stepwise transitions described above are related to the pH-dependent conformational flexibility of the pore structural constituents (Hess et al., 1989) rather than to the direct interaction between the fluctuating charges of the channel residues and the current-carrying ions.

The rate of the flickering (number of events per second, n) can be calculated using the equation (Nestorovich et al., 2002),

$$n = \frac{S(0)}{4(\Delta i)^2 \tau^2}. \tag{4}$$

Fig. 8 B shows this rate as a function of pH. A linear dependence (*straight dashed line*) is expected in the case of direct interaction between the independently fluctuating charges of the channel residues with $pK_a < 2$ and the permeant ions. The actual dependence is slightly superlinear in proton concentration, $n \propto [H^+]^{1.3}$ (*solid line* through the data).

Results of noise spectral measurements at pH 8.0, where the time-resolved transients are not detectable, are shown in Fig. 9. Each spectrum can be represented by a sum of a Lorentzian and the background spectrum. It is worth emphasizing that in the whole range of pH studied here, channel noise was free from *1/f* fluctuations. Both time-resolved stepwise transients seen in acidic solutions and fast conductance fluctuations in basic solutions produce spectra of a simple relaxation type. This is in a sharp contrast with the observations made for Maltoporin channel where currents display much more complex dynamics and, as a result,
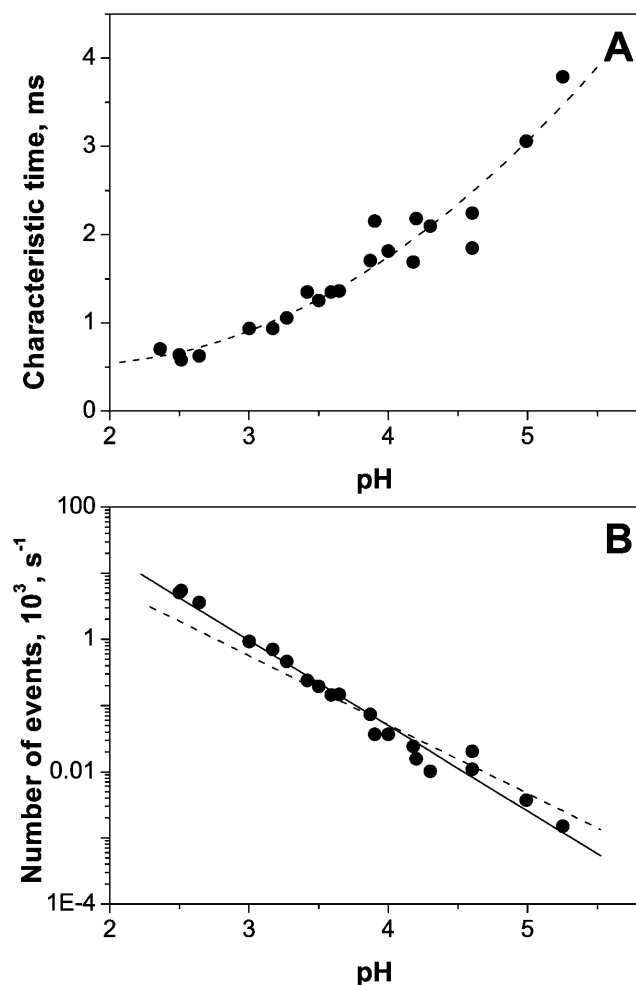
FIGURE 8 (A) The characteristic time of the noise produced by the stepwise transients, τ, obtained by fitting Eq. 1 to noise spectra, depends on the bathing solution pH. At pH $\sim$ 5.3 it is close to 4 ms. Changing pH from 5.3 to 2.5 causes more than fourfold decrease in the characteristic time. (B) The frequency of the transients (number of events per second) increases with proton concentration. Bathing solution was 1 M KCl. Applied voltage was 100 mV.
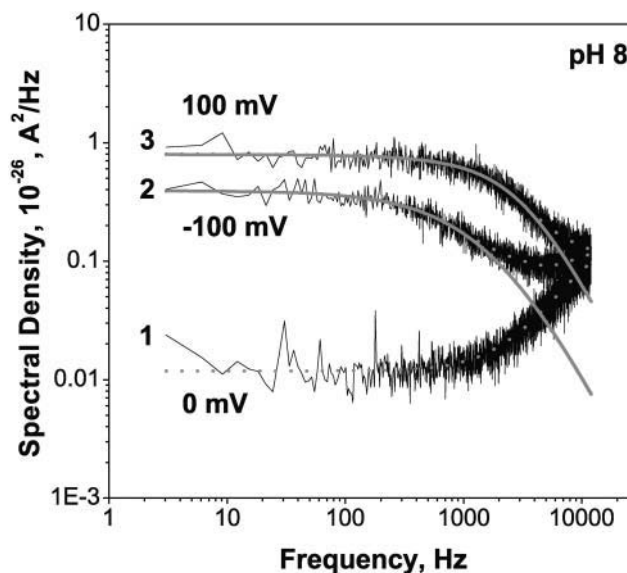

FIGURE 9 Power spectral density and corner frequency of noise in the current through a single fully open channel depend on the applied voltage. The difference spectra, obtained by subtracting the background spectrum measured at 0 mV (curve 1), are described by Lorentzians (solid lines) with characteristic times of $\sim$0.2 ms for –100 mV (curve 2) and 0.07 ms for 100 mV (curve 3). Bathing solution was 1 M KCl.

open channel noise is dominated by the 1/f spectral component (Bezrukov and Winterhalter, 2000).

Fig. 9 also illustrates that both the low-frequency spectral density and the characteristic cutoff frequency of the open channel noise depend on the applied voltage. Noise is higher and more broadband at positive potentials. This asymmetry in voltage is pH-dependent. Fig. 10 illustrates this for pH 8.0 and pH 3.9.

It is well-known that OmpF transport properties are governed by an internal constriction consisting of the negatively charged loop 3 folded into the channel lumen and the positively charged barrel wall located on the opposite site across the pore, "anti-loop 3" (Bredin et al., 2002; Phale et al., 2001, 1997). This unusual organization of the pore eyelet, with two half-rings of opposite charge situated face to face in a restricted space, generates an intense electrostatic field in the pore (Karshikoff et al., 1994).

Up to now, several residues of L3 have been shown to be involved in channel activity, such as Asp-113 and Glu-117, which participate in the architecture of the negative cluster at loop L3 (Karshikoff et al., 1994; Phale et al., 1997). In particular, mutations D113C and E117C decrease OmpF single channel conductance by 17 $\pm$ 10% and 24 $\pm$ 8%, respectively (Van Gelder et al., 1997; Phale et al., 2001). These values are close to 19% and 21% differences between the maximum current of the fully open channel and the current of the smaller conductance substates reported here (see Figs. 4 and 5). Based on this, it is tempting to attribute the stepwise downward current transients observed at low pH to the reversible protonation of Asp-113 and Glu-117 at the internal loop L3. Moreover, D113G mutant loses cationic selectivity of the wild-type porin (P_{Na}/P_{Cl} ratio of 1.4 $\pm$ 0.1 as compared to 4.5 $\pm$ 0.8; Saint et al., 1996). This finding again is in good agreement with the decrease in cationic selectivity of wild-type OmpF (Fig. 3 B) at the low solution pH where carboxyl side chains of Asp-113 and Glu-117 appear to be mostly protonated.

Several residues belonging to the anti-loop 3 have been characterized functionally (Bredin et al., 2002; Benson et al., 1988; Saint et al., 1996; Lou et al., 1996). Continuum electrostatic calculations (Karshikoff et al., 1994), suggest that the three arginine residues (42, 82, and 132) that are stacked next to each other at the pore constriction show abnormal titration behavior. Namely, Arg-82 experiences an
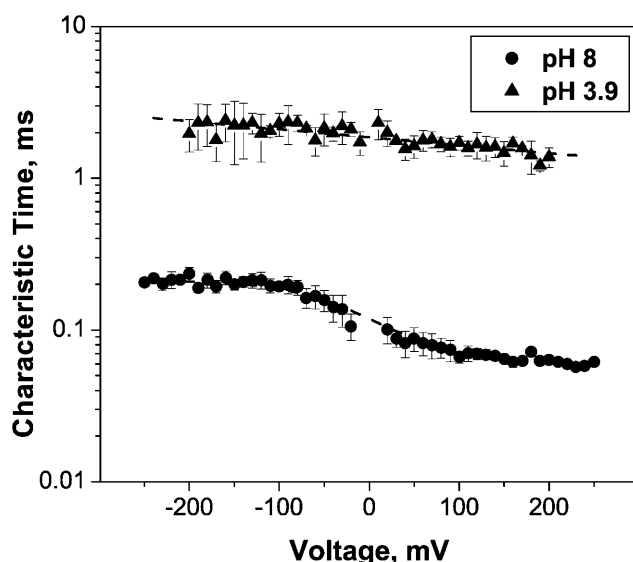
FIGURE 10 The characteristic time of the open channel noise in both basic (pH 8) and acidic (pH 3.9) 1 M KCl solutions as functions of the applied voltage. Even though the characteristic times of these two process differ by an order of magnitude ($0.06 \div 0.2$ ms at pH 8 and $1.5 \div 2.5$ ms at pH 3.9), both curves show similar voltage asymmetry, giving 70% (pH 8) and 40% (pH 3.9) higher values at –200 mV than at 200 mV.

enormous pK shift (to pK < 3), so that it is uncharged at neutral pH whereas pK values for Arg-42 and Arg-132 exceed 13. The results obtained for R42C, R82C, and R132P mutants showed some minor decrease in single OmpF channel conductance together with evident increase in Na^+ permeability (Saint et al., 1996).

Lys-16 with pK 11.3 (Karshikoff et al., 1994) is one more distal residue of the anti-loop 3 basic cluster facing Glu-117 at the loop 3. It is interesting that substitution K16D causes some increase ($\sim$7%) in single OmpF channel conductance as well as double increase in Na^+ permeability as compared with wild-type (P_{Na}/P_{Cl} ratio of 10.2 ± 0.9 for K16D mutant vs. 4.2 ± 0.9 for wild-type; Bredin et al., 2002). Thus, Lys-16, which deprotonates at lower pH values compared to the arginine cluster, seems to be a better candidate to explain the effects observed for basic electrolyte solutions.

Furthermore, in addition to the main source of electrostatic field across the constriction zone that is formed by basic cluster (Arg-42, Arg-82, Arg-132, Lys-16) on the barrel wall and the two carboxyl side chains (Asp-113, Glu-117) on the loop 3, several other residues have been shown to influence the OmpF transport properties (Karshikoff et al., 1994; Iyer et al., 2000; Bainbridge et al., 1998a). For instance, substitutions G119D and G119E lead to noticeable colicin resistance, drastic alteration in diffusion and antibiotic susceptibility, and structural changes inside the lumen (Bredin et al., 2002; Jenteur et al., 1994; Simonet et al., 2000). Besides, there are a number of ionizable groups deeply buried inside the protein and thus exhibiting large pK shifts (for details see Table 1 in Karshikoff et al., 1994).

These groups may be partially responsible for the decrease in the maximum conductance seen in Fig. 4 and for the high-frequency noise of the current through the open channel.

Direct electric field effects versus pH-induced structural changes

Our main findings demonstrate that both the maximal, time-resolved channel conductance (Fig. 4) and the average channel conductance (Fig. 3 A) are the decreasing functions of proton concentration. Can this conductance reduction be entirely attributed to the direct interaction of the permeating ions with the pH-dependent charges of ionizable residues of the channel pore? Or, alternatively, should we rather think about some pH-dependent changes in the structure of the pore that reduce its diameter? The latter idea had been advanced by Todt and colleagues (Todt et al., 1992; Todt and McGroarty, 1992) who deduced channel size from the "channel conductance/bulk conductance" ratio using notion of a cylinder filled with solution of the same conductivity as the bulk. In an attempt to answer these questions, we studied partitioning of a water-soluble polymer, polyethyleneglycol, with a molecular weight of 1000 Da (PEG 1000), into the channel pore at different pH.

Recently we have shown (Rostovtseva et al., 2002) that the characteristic polymer cutoff size of PEG partitioning into the pores of OmpF and α-hemolysin correlates nicely with the effective pore radii calculated from the high-resolution x-ray structures of these channels (Cowan et al., 1992; Dutzler et al., 1999; Song et al., 1996). This finding further supports polymer partitioning as a tool for sizing channel pores in their functional states (Krasilnikov et al., 1992; 1998; Bezrukov and Vodyanoy, 1993; Bezrukov et al., 1994, 1996; Bezrukov and Kasianowicz, 2001; Krasilnikov, 2002). Here we apply this method in an attempt to understand whether the OmpF conductance reduction at high proton concentrations is accompanied by a decrease in the geometrical size of the channel pore.

Main results of polymer partitioning experiments are presented in Fig. 11. PEG 1000 was chosen because partitioning of this polymer is expected to be most sensitive to the changes in the OmpF pore size. In experiments with PEG of varying molecular weight w, it was found (Rostovtseva et al., 2002) that in the case of OmpF the molecular-weight-dependent partition coefficient $p(w)$ could be described by

$$p(w) = \exp[-(w/w_0)^{\alpha}], \quad (5)$$

where $\alpha = 1.65$ and $w_0 = 1360$. Therefore, molecular weight of 1000 Da represents roughly the midpoint of the transition between polymer exclusion, where addition of polymers does not influence channel conductance, and their free partitioning, where addition of polymers reduces channel conductance by approximately the same ratio as solution conductivity.
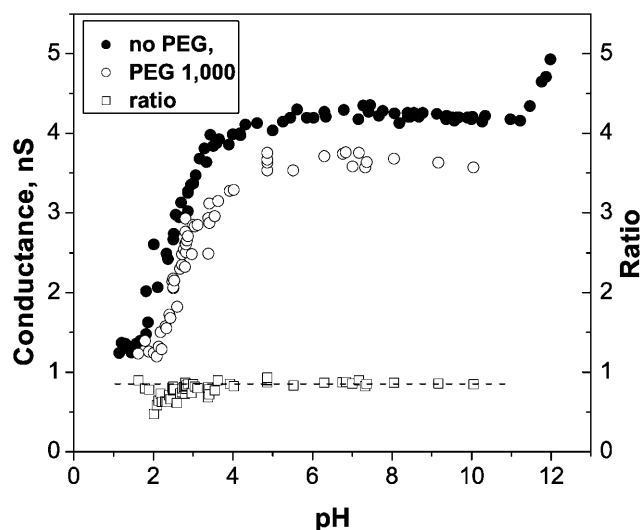
FIGURE 11   Addition of 15% (w/w) PEG 1000 to the membrane-bathing solution of 1 M KCl decreases channel conductance over the whole pH range studied (*unfilled circles*, 100 mV of applied voltage). Solid circles represent data for the OmpF conductance in pure KCl solutions (Fig. 3 *A*, *solid circles*). Unfilled squares are the ratio of channel conductance in the presence of polymer to its conductance in polymer-free solutions. The horizontal dotted line is drawn as the average ratio over the pH range of the conductance plateau, from pH 5.0 to pH 9.0.

It is seen that addition of PEG 1000 reduces channel conductance over the whole range of solution acidities. Importantly, the ratio of channel conductance in the presence of polymer to its conductance in polymer-free solution does not seem to increase with the increasing proton concentration up to pH 2.0. This observation does not support the idea of pore diameter reduction as the cause of the conductance decrease, because for a smaller pore one would expect a smaller polymer effect.

Thus, polymer-partitioning experiments suggest that the protonation of the ionizable residues changes electric potential distribution in the channel pore without significant changes in its geometry. The tentative tone of our conclusion is related to the fact that in the most interesting pH range (from pH 1 to pH 4) the channel conductance is a very steep function of solution acidity (Figs. 3 *A* and 11). Here the channel conductance is highly sensitive to the residue charge state, which, in its own turn, is sensitive to the dielectric constant of the immediate environment. Addition of PEG changes the dielectric constant of the membrane-bathing solution and, due to finite PEG penetration, the dielectric constant of the solution inside the pore. Therefore, the pK_a values of the channel residues could be slightly shifted relatively to their values in polymer-free solution, which would make the comparison of the two curves difficult.

It is worth emphasizing that even for large channels their conductance is a poor measure of the pore size. The absence of a simple correlation between the channel pore size and the single-channel conductance was realized many years ago (Finkelstein, 1985). Recent studies confirm this observation

and search for possible explanations (Smart et al., 1997; Tieleman and Berendsen, 1998; Phale et al., 2001; Rostovtseva et al., 2002).

CONCLUSIONS

OmpF channels reconstituted in planar bilayer membranes can endure extreme pH conditions for hours. Exposed to highly acidic or basic environments of pH 1 or pH 12, they can be returned to their completely functional state when solution pH is brought back to neutral. This robustness makes it possible to study channel transport properties over a broad range of solution pH. We find that:

- Conductance of the channel in its fully open state displays three characteristic regimes. Under acidic conditions conductance strongly depends on solution pH, increasing threefold when pH is increased from pH 1.0 to pH 5. At neutral pH it displays a plateau that extends from pH 5 to pH 9. In basic solutions, from pH 9 to pH 12, channel conductance is again pH-sensitive and increases by 15–30%, depending on the sign of the applied voltage.
- Channel selectivity is also pH-dependent and its behavior resembles that of the channel conductance. It has a plateau over pH 5 to pH 9 corresponding to cationic selectivity of $t_K^+ \approx 3t_{Cl}^-$, with a slight increase in basic solutions at pH 9.5 to pH 12. In acidic solutions, cationic selectivity decreases; at pH $\leq$ 3.5, the channel becomes anion-selective. By pH 2, channel selectivity is $t_{Cl}^- \approx 3t_K^+$.
- Analysis of open channel noise and stepwise time-resolved transients in the open state demonstrates that at least three different ionization processes are involved in the pH-dependent modification of the channel transport properties. Noise is minimal in the pH range corresponding to the conductance and selectivity plateaus, but it is still much higher than the Johnson or shot noise expected for these conductances and currents.
- Polymer-partitioning experiments suggest that the conductance reduction in solutions of high acidity is not accompanied by the geometrical reduction of the pore diameter. This observation is in favor of direct electrostatic interactions between the channel residues and the penetrating ions as the cause of the observed pH dependence of ion transport.

REFERENCES

Bainbridge, G., H. Mobasheri, G. A. Armstrong, E. J. A. Lea, and J. H. Lakey. 1998a. Voltage-gating of *E. coli* porin: a cystine-scanning mutagenesis study of loop 3. *J. Mol. Biol.* 275:171–176.

Bainbridge, G., I. Gokce, and J. H. Lakey. 1998b. Voltage gating is a fundamental feature of porin and toxin β-barrel membrane channels. *FEBS Lett.* 431:305–308.

Bayley, H., and P. S. Cremer. 2001. Stochastic sensors inspired by biology. *Nature.* 413:226–230.

Benson, S. A., J. L. Occi, and B. A. Sampson. 1988. Mutations that alter the pore function of the OmpF porin of *E. coli* K12. *J. Mol. Biol.* 203:961–970.

Benz, R., and K. Bauer. 1988. Permeation of hydrophilic molecules through the outer membrane of gram-negative bacteria. Review on bacterial porins. *Eur. J. Biochem.* 176:1–19.

Benz, R., K. Janko, W. Boos, and P. Lauger. 1978. Formation of large, ion-permeable membrane channels by the matrix protein (porin) of *E. coli.* *Biochim. Biophys. Acta.* 511:305–319.

Benz, R., K. Janko, and P. Lauger. 1979. Ionic selectivity of pores formed by the matrix protein (porin) of *E. coli. Biochim. Biophys. Acta.* 551:238–247.

Bezrukov, S. M. 2000. Ion channels as molecular Coulter counters to probe metabolite transport. *J. Membr. Biol.* 174:1–13.

Bezrukov, S. M., and J. J. Kasianowicz. 1993. Current noise reveals protonation kinetics and number of ionizable sites in an open protein ion channel. *Phys. Rev. Lett.* 70:2352–2355.

Bezrukov, S. M., and J. J. Kasianowicz. 2001. Neutral polymers in the nanopores of alamethicin and alpha-hemolysin. *Biol. Membr.* 18:453–457.

Bezrukov, S. M., L. Kullman, and M. Winterhalter. 2000. Probing sugar translocation through maltoporin at the single channel level. *FEBS Lett.* 476:224–228.

Bezrukov, S. M., and I. Vodyanoy. 1993. Probing alamethicin channels with water-soluble polymers. Effect on conductance of channel states. *Biophys. J.* 64:16–25.

Bezrukov, S. M., I. Vodyanoy, and V. A. Parsegian. 1994. Counting polymers moving through a single ion channel. *Nature.* 370:279–281.

Bezrukov, S. M., I. Vodyanoy, R. A. Brutyan, and J. J. Kasianowicz. 1996. Dynamics and free energy of polymers partitioning into a nanoscale pore. *Macromolecules.* 29:8517–8522.

Bezrukov, S. M., and M. Winterhalter. 2000. Examining noise sources at the single-molecule level: 1/f noise of an open maltoporin channel. *Phys. Rev. Lett.* 85:202–205.

Bredin, J., N. Saint, M. Malléa, E. De, G. Molle, J.-M. Pagés, and V. Simonet. 2002. Alteration of pore properties of *E. coli* OmpF induced by mutation of key residues in anti-loop 3 region. *Biochem. J.* 363:521–528.

Chevalier, J., M. Malléa, and J.-M. Pagés. 2000. Comparative aspects of the diffusion of norfloxacin, cefepime and spermine through the F porin channel of *Enterobacter cloacae. Biochem. J.* 348:223–227.

Cowan, S. W., T. Schirmer, G. Rummel, M. Steiert, R. Ghosh, R. A. Pauptit, J. N. Jansonius, and J. P. Rosenbusch. 1992. Crystal structures explain functional properties of two *E. coli* porins. *Nature.* 358:727–733.

Delcour, A. H. 2003. Solute uptake through general porins. *Frontiers Biosci.* 8:1055–1071.

Delcour, A. H. 2002. Structure and function of pore-forming β-barrels from bacteria. *J. Mol. Microbiol. Biotechnol.* 4:1–10.

Dutzler, R., G. Rummel, S. Alberti, S. Hernández-Allés, P. S. Phale, J. P. Rosenbusch, V. J. Benedi, and T. Schirmer. 1999. Crystal structure and functional characterization of OmpK36, the osmoporin of *Klebsiella pneumoniae. Struct. Fold. Des.* 7:425–434.

Finkelstein, A. 1985. The ubiquitous presence of channels with wide lumens and their gating by voltage. *Ann. N. Y. Acad. Sci.* 456:26–32.

Hess, P., B. Prod'hom, and D. Pietrobon. 1989. Mechanisms of interaction of permeant ions and protons with dihydropyridine-sensitive calcium channels. *Ann. New York Acad. Sci.* 560:80–93.

Im, W., and B. Roux. 2002. Ion permeation and selectivity of OmpF porin: a theoretical study based on molecular dynamics, Brownian dynamics, and continuum electrodiffusion theory. *J. Mol. Biol.* 322:851–869.

Im, W., S. Seefeld, and B. Roux. 2000. A grand canonical Monte Carlo-Brownian dynamics algorithm for simulating ion channels. *Biophys. J.* 79:788–801.

Iyer, R., Z. Wu, P. M. Woster, and A. H. Delcour. 2000. Molecular basis for the polyamine-OmpF porin interaction: inhibitor and mutant studies. *J. Mol. Biol.* 297:933–945.

Jeanteur, D., T. Schirmer, D. Fourel, V. Simoner, G. Rummel, C. Widmer, J. P. Rosenbusch, F. Pattus, and J. M. Pages. 1994. Structural and functional alterations of a colicin-resistant mutant of OmpF porin from *E. coli. Proc. Natl. Acad. Sci. USA.* 91:10675–10679.

Karshikoff, A., V. Spassov, S. W. Cowan, R. Ladenstein, and T. Schirmer. 1994. Electrostatic properties of two porin channels from *E. coli. J. Mol. Biol.* 240:372–384.

Kasianowicz, J. J., and S. M. Bezrukov. 1995. Protonation dynamics of the α-toxin ion channel from spectral analysis of pH-dependent current fluctuations. *Biophys. J.* 69:94–105.

Kasianowicz, J. J., E. Brandin, D. Branton, and D. W. Deamer. 1996. Characterization of individual polynucleotide molecules using a membrane channel. *Proc. Natl. Acad. Sci. USA.* 93:13770–13773.

Klebba, P. E., and S. M. Newton. 1998. Mechanisms of solute transport through outer membrane porins: burning down the house. *Curr. Opin. Microbiol.* 1:238–247.

Kobayashi, Y., and T. Nakae. 1985. The mechanism of ion selectivity of OmpF-porin pores of *E. coli. Eur. J. Biochem.* 151:231–236.

Koebnik, R., K. P. Locher, and P. Van Gelder. 2000. Structure and function of bacterial outer membrane proteins: barrel in a nutshell. *Mol. Microbiol.* 37:239–253.

Krasilnikov, O. V., R. Z. Sabirov, V. I. Ternovsky, P. G. Merzliak, and J. N. Muratkhodjaev. 1992. A simple method for the determination of the pore radius of ion channels in a planar lipid bilayer membranes. *FEMS Microbiol. Immunol.* 5:93–100.

Krasilnikov, O. V., J. B. Da Cruz, L. N. Yuldasheva, and R. A. Nogueira. 1998. A novel approach to study the geometry of the water lumen of ion channels: colicin Ia channels in planar lipid bilayers. *J. Membr. Biol.* 161:83–92.

Krasilnikov, O. V. 2002. Sizing channels with polymers. *In* Structure and Dynamics of Confined Polymers. J. J. Kasianowicz, M. S. Z. Kellermayer, and D. W. Deamer, editors. Kluwer Publishers. Dordrecht, The Netherlands. 97–115.

Kreusch, A., and G. E. Schultz. 1994. Refined structure of the porin from *Rhodopseudomonas blastica* and comparison with the porin from *Rhodobacter capsulatus. J. Mol. Biol.* 243:891–905.

Kullman, L., M. Winterhalter, and S. M. Bezrukov. 2002. Transport of maltodextrins through maltoporin: a single-channel study. *Biophys. J.* 82:803–812.

Li, J., D. Stain, C. McMullan, D. Branton, M. J. Aziz, and J. A. Golovchenko. 2001. Ion-beam sculpting at nanometre length scales. *Nature.* 412:166–169.

Liu, N., and A. Delcour. 1998. Inhibitory effect of acidic pH on OmpC porin: wildtype and mutant studies. *FEBS Lett.* 434:160–164.

Lou, K. L., N. Saint, A. Prolipov, G. Rummel, S. A. Benson, J. P. Rosenbusch, and T. Schirmer. 1996. Structural and functional characterization of OmpF porin mutants selected for larger pore size. I. Crystallographic analysis. *J. Biol. Chem.* 271:20669–20675.

Meller, A. 2003. Dynamics of polynucleotide transport through nanometer-scale pore. *J. Phys. Condens. Matter.* 15:R581–R607.

Meller, A., and D. Branton. 2002. Single molecule measurements of DNA transport through a nanopore. *Electrophoresis.* 23:2583–2591.

Montal, M., and P. Mueller. 1972. Formation of bimolecular membranes from lipid monolayers and study of their electrical properties. *Proc. Natl. Acad. Sci. USA.* 69:3561–3566.

Müller, D. J., and A. Engel. 1999. Voltage and pH-induced channel closure of porin OmpF visualized by atomic force microscopy. *J. Mol. Biol.* 285:1347–1351.

Nestorovich, E. M., C. Danelon, M. Winterhalter, and S. M. Bezrukov. 2002. Designed to penetrate: time-resolved interaction of single

antibiotic molecules with bacterial pores. *Proc. Natl. Acad. Sci. USA.* 99:9789–9794.

Nikaido, H., and M. Vaara. 1985. Molecular basis of bacterial outer membrane permeability. *Microbiol. Rev.* 49:1–32.

Nikaido, H. 1992. Porins and specific channels of bacterial outer membranes. *Mol. Microbiol.* 6:435–442.

Phale, P. S., A. Philippsen, C. Widmer, V. P. Phale, J. P. Rosenbusch, and T. Schirmer. 2001. Role of charged residues at the OmpF porin channel constriction probed by mutagenesis and simulation. *Biochemistry.* 40:6319–6325.

Phale, P. S., A. Philippsen, T. Kiefhaber, R. Koebnik, V. P. Phale, T. Schirmer, and J. P. Rosenbusch. 1998. Stability of trimeric OmpF porin: the contribution of the latching loop L2. *Biochemistry.* 37:15663–15670.

Phale, P. S., T. Schirmer, A. Prilipov, K.-L. Lou, A. Hardmeyer, and J. P. Rosenbusch. 1997. Voltage gating of *E. coli* porin channels: role of the constriction loop. *Proc. Natl. Acad. Sci. USA.* 94:6741–6745.

Philippsen, A., W. Im, A. Engel, T. Schirmer, B. Roux, and D. J. Müller. 2002. Imaging the electrostatic potential of transmembrane channels: atomic probe microscopy of OmpF porin. *Biophys. J.* 82:1667–1676.

Prod'hom, B., D. Pietrobon, and P. Hess. 1987. Direct measurement of proton transfer rates to a group controlling the dihydropyridine-sensitive Ca^{2+} channel. *Nature.* 329:243–246.

Robertson, K. M., and D. P. Tieleman. 2002a. Molecular basis of voltage gating of OmpF porin. *Biochem. Cell Biol.* 80:517–523.

Robertson, K. M., and D. P. Tieleman. 2002b. Orientation and interactions of dipolar molecules during transport through OmpF porin. *FEBS Lett.* 528:53–57.

Rostovtseva, T. K., and S. M. Bezrukov. 1998. ATP transport through a single mitochondrial channel, VDAC, studied by current fluctuation analysis. *Biophys. J.* 74:2365–2373.

Rostovtseva, T. K., T.-T. Liu, M. Colombini, V. A. Parsegian, and S. M. Bezrukov. 2000. Positive cooperativity without domains or subunits in a monomeric membrane channel. *Proc. Natl. Acad. Sci. USA.* 97:7819–7822.

Rostovtseva, T. K., E. M. Nestorovich, and S. M. Bezrukov. 2002. Partitioning of differently sized poly(ethylene glycol)s into OmpF porin. *Biophys. J.* 82:160–169.

Saint, N., K. L. Lou, C. Widmer, M. Luckey, T. Schirmer, and J. P. Rosenbusch. 1996. Structural and functional characterization of OmpF porin mutants selected for larger pore size. II. Functional characterization. *J. Biol. Chem.* 271:20676–20680.

Saleh, O. A., and L. L. Sohn. 2003. Direct detection of antibody-antigen binding using an on-chip artificial pore. *Proc. Natl. Acad. Sci. USA.* 100:820–824.

Schindler, H., and J. P. Rosenbusch. 1978. Matrix protein from *E. coli* outer membranes forms voltage-controlled channels in lipid bilayers. *Proc. Natl. Acad. Sci. USA.* 75:3751–3755.

Schindler, H., and J. P. Rosenbusch. 1981. Matrix protein in planar membranes: clusters of channels in a native environment and their functional reassembly. *Proc. Natl. Acad. Sci. USA.* 78:2302–2306.

Schirmer, T., and P. S. Phale. 1999. Brownian dynamics simulation of ion flow through porin channels. *J. Mol. Biol.* 294:1159–1167.

Simonet, V., M. Malléa, and J.-M. Pagés. 2000. Substitutions in the eyelet region disrupt cefepime diffusion through the *E. coli* OmpF channel. *Antimicrob. Agents Chemother.* 44:311–315.

Smart, O. S., J. Breed, G. R. Smith, and M. S. Sansom. 1997. A novel method for structure-based prediction of ion channel conductance properties. *Biophys. J.* 72:1109–1126.

Song, L., M. R. Hobaugh, C. Shustak, S. Cheley, H. Bayley, and J. E. Gouaux. 1996. Structure of staphylococcal α-hemolysin, a heptameric transmembrane pore. *Science.* 274:1859–1866.

Suenaga, A., Y. Komeiji, M. Uebayasi, T. Meguro, M. Saito, and I. Yamato. 1998. Computational observation of an ion permeation through a channel protein. *Biosci. Rep.* 18:39–48.

Tieleman, D. P., and H. J. Berendsen. 1998. A molecular dynamics study of the pores formed by *E. coli* OmpF porin in a fully hydrated palmitoyloleoylphosphatidylcholine bilayer. *Biophys. J.* 74:2786–2801.

Todt, J. C., W. J. Rocque, and E. J. McGroarty. 1992. Effects of pH on bacterial porin function. *Biochemistry.* 31:10471–10478.

Todt, J. C., and E. J. McGroarty. 1992. Acid pH decreases OmpF and OmpC channel size *in vivo. Biochem. Biophys. Res. Commun.* 189:1498–1502.

Urban, B. W., S. B. Hladky, and D. A. Haydon. 1980. Ion movements in gramicidin pores. An example of single-file transport. *Biochim. Biophys. Acta.* 602:331–354.

Van Gelder, P., F. Dumas, and M. Winterhalter. 2000. Understanding the function of bacterial outer membrane channels by reconstitution into black lipid membranes. *Biophys. Chem.* 85:153–167.

Van Gelder, P., N. Saint, P. Phale, E. F. Eppens, A. Prilipov, R. van Boxtel, and J. P. Rosenbusch. 1997. Voltage sensing in the PhoE and OmpF outer membrane porins in of *E. coli*: role of charged residues. *J. Mol. Biol.* 269:468–472.

Watanabe, M., J. Rosenbusch, T. Shirmer, and M. Karplus. 1997. Computer simulations of the OmpF porin from the outer membrane of *E. coli. Biophys. J.* 72:2094–2102.

Weiss, M. S., T. Wacker, J. Weckesser, W. Welte, and G. E. Schulz. 1990. The three-dimensional structure of porin from *Rhodobacter capsulatus* at 3 Å resolution. *FEBS Lett.* 267:268–272.

Xu, G., B. Shi, E. J. McGroarty, and H. T. Tien. 1986. Channel-closing activity of porins from *E. coli* in bilayer lipid membranes. *Biochim. Biophys. Acta.* 862:57–64.

Yoshimura, F., and H. Nikaido. 1985. Diffusion of β-lactam antibiotics through the porin channels of *E. coli* K-12. *Antimicrob. Agents Chemother.* 27:84–92.